2.5-D fluid simulations of the solar wind interacting with multiple dipoles on the surface of the Moon

Erika M. Harnett and Robert M. Winglee

Department of Earth and Space Sciences, University of Washington, Seattle, Washington, USA

Received 30 July 2002; revised 9 October 2002; accepted 15 October 2002; published 21 February 2003.

[1] Initial two-dimensional (2-D) MHD simulations indicated that mini-magnetospheres can form around magnetic anomalies on the surface of the Moon but required magnetic field strengths at 100 km above the surface an order of magnitude larger than in situ measurements. Modeling the lunar magnetic anomalies with multiple dipoles in 2.5-D MPD simulations inflates the size of the mini-magnetospheres for only small increases in the magnitude of the total magnetic field. Multiple dipoles increase the lateral distance over which solar wind plasma is held off the surface. This extended magnetic field geometry inflates the mini-magnetosphere by inhibiting fluid flow within the shock region. With multiple dipoles, a mini-magnetosphere will form with magnetic field magnitudes smaller than the lower limit for a single dipole. These results indicate that the higher order moments of the anomalous magnetic fields play a significant role in deflecting the solar wind and determining the size and shape of the mini-magnetosphere. *INDEX TERMS:* 6250 Planetology: Solar System Objects: Moon (1221); 2753 Magnetospheric Physics: Numerical modeling; 2756 Magnetospheric Physics: Planetary magnetospheres (5443, 5737, 6030); 2784 Magnetospheric Physics: Solar wind/magnetosphere interactions; 6030 Planetology: Comets and Small Bodies: Magnetic fields and magnetism; *KEYWORDS:* mini-magnetospheres, Moon, MHD, numerical simulation, magnetic anomalies

Citation: Harnett, E. M., and R. M. Winglee, 2.5-D fluid simulations of the solar wind interacting with multiple dipoles on the surface of the Moon, *J. Geophys. Res.*, *108*(A2), 1088, doi:10.1029/2002JA009617, 2003.

1. Introduction

[2] Two-dimensional (2-D) MHD simulations of the solar wind interaction with the lunar magnetic anomalies [*Harnett and Winglee*, 2000] indicated that the crustal magnetic fields can hold off the solar wind and form a ''mini-magnetosphere'' (a small-scale magnetosphere). A mini-magnetosphere would form in the 2-D MHD simulations when a dipole buried 50 km below the surface had a surface field strength of 290 nT at the surface and greater than 10 nT at 100 km above the surface, for solar wind velocity and density equal to 400 km s^{-1} and 10 cm^{-3}, respectively. When the velocity was 400 km/s and the magnetic anomaly was 290 nT at the surface and 30 nT at 100 km, a mini-magnetosphere formed for solar wind densities less than 40 cm^{-3}. The 2-D MHD results also indicated that mini-magnetospheres are much more dynamic than planetary sized magnetospheres. Simply flipping the direction of the IMF from southward to northward caused the mini-magnetosphere to double in size and change from an elongated shock surface to a round shock surface.

[3] One inconsistency arose from the comparison of the 2-D MHD simulations and observations of possible mini-magnetospheres made by Lunar Prospector [*Lin et al.*, 1998]. The strength of the magnetic field at 100 km above the surface needed to be an order of magnitude larger than values observed by Lunar Prospector in order for mini-magnetospheres to form at satellite altitudes. Lunar Prospector found that in the lunar wake the in situ field strengths above the anomalies that had shock-like structures when facing into the solar wind were on the order of a few nanotesla (R. Lin et al., private communication, 1999 and L. L. Hood, private communication, 2001). In the initial simulations the field strength at 100 km above the surface dipole had to be set to approximately 30 nT in order for a mini-magnetosphere to form at satellite altitudes.

[4] The extra currents and electric fields that arose from extending the model to nonideal MHD, incorporating small-scale effects [*Harnett and Winglee*, 2002], did add extra features to the mini-magnetosphere and allowed for a better understanding of the physical processes occurring, but they caused no inflation of the mini-magnetosphere. Some other mechanism is needed to cause a mini-magnetosphere to form at higher altitudes with smaller anomalous magnetic fields.

[5] The larger than observed anomalous magnetic field strength required at 100 km may be due to modeling the anomalous magnetic field with a simple dipole. The outermost shock surfaced formed between 100 to 200 km above the surface with the lateral extent of the mini-magnetospheres approximately an order of magnitude larger. With plasma and magnetic field interactions occurring close to the source region of the anomalous magnetic field, a single dipole approximation is likely to breakdown. The strength

0148-0227/03/2002JA009617

of the higher-order terms could be comparable to the strength of the dipole term when considering a more realistic model of the crustal magnetic field.

[6] The results presented in this paper show the effects of modeling anomalous magnetic fields as a collection of dipoles rather than a single dipole and how a complex magnetic field geometry modifies the plasma dynamics. It is also an intermediate step necessary for creating realistic magnetic fields in 3-D simulations. Different methods can be used to model the individual anomalies, such as multiple dipoles or spherical harmonics. A multiple dipole technique was used by *Hood and Williams* [1989] to model anomalies on the Moon. In their simulations, 9–15 dipoles were used to create a source region approximately 200 km by 200 km with field strengths on the order of 1000 nT at the surface and 2 nT at 100 km above the surface.

[7] Not only does the study of mini-magnetospheres provide new physical insight into lunar processes, the results could lend insight into unresolved issues arising from data taken during the Apollo missions. Solar wind measurements made on the lunar surface by the ALSEP instrument [*Neugebauer et al.*, 1972; *Freeman*, 1972] showed possible modulation of the incident ions by nearby magnetic anomalies. *Hood and Williams* [1989] proposed that such modulation could explain the variation in surface albedo near anomalous regions, for example the markings near Reiner Gamma. Such modulation could affect chemical composition of the surface the surface. *Hood and Williams* [1989] suggested that regions where the solar wind is deflected would reduce the deposition of hydrogen, leading to a surface that has not been darkened by impact of solar wind particles. This shielding of the surface from space weathering at the Moon could provide a source of material that has been subject to primarily galactic radiation exposure. At Mars, the anomalous regions could supplement the partial shielding of cosmic rays provided by the atmosphere.

2. Model Parameters

[8] The simulations with the multiple dipoles were run with the same initial conditions as previous simulations [*Harnett and Winglee*, 2000, 2002]. The following fluid equations are solved using the two-step Lax-Wendroff finite difference method [*Richtyer and Morton*, 1967], which is second order correct:

$$\frac{\partial \rho}{\partial t} + \nabla \cdot \vec{m} = 0 \tag{1}$$

$$\frac{\partial \vec{m}}{\partial t} + \nabla \cdot \left(\vec{m} \frac{\vec{m}}{\rho} \right) + \nabla P = \vec{J} \times \vec{B} \tag{2}$$

$$\frac{\partial e}{\partial t} + \nabla \cdot \left(\frac{\vec{m}}{\rho} (e + P) \right) = \vec{E} \cdot \vec{J} \tag{3}$$

$$\frac{\partial \vec{B}}{\partial t} - \nabla \times \vec{E} = 0 \tag{4}$$

$$\vec{J} = \nabla \times \vec{B} \tag{5}$$

$$\vec{E} = -\vec{v} \times \vec{B} + \eta \vec{J} + \frac{1}{q n_i} \left(\vec{J} \times \vec{B} - \nabla P_e \right), \tag{6}$$

where $\vec{E}$ is the electric field, $\vec{B}$ is the magnetic field, $\vec{J}$ is the current density, P_e is the electron pressure (and equal to half the total pressure, P), e is the energy density, $\vec{m}$ is the momentum, ρ is the density, η is resistivity, q is charge, and n_i is ion number density. The resistivity (η) is set to zero outside of the Moon, and the Hall and ∇P_e terms (that account for nonideal MHD behavior and regions of localized nonneutrality) are only evaluated outside of the Moon. The vector quantities are three component vectors, but the spatial derivatives are only taken in two dimensions.

[9] The solar wind was assumed to be composed of H^+ ions with a density of 10 cm^{-3} and a velocity of 400 km s^{-1}. The lunar density was assumed to be 0.1 Ar^+ cm^{-3} on the dayside and 0.01 on the nightside [*Johnson*, 1971; *Hodges*, 1974]. The ion density can not be set to zero at the lunar surface as it would introduce division by zero. The lunar density is low enough that the surface acts as a sink for undeflected solar wind. These 2.5-D MPD simulations are a one ion species code, so an Ar^+ ion is treated as 40 H^+ ions.

[10] The pressure and temperature of the solar wind are equal to 0.02 nPa and 12 eV, respectively. The IMF was set to 2.5 nT in the southward direction ($-\hat{z}$), and the resistivity of the Moon was set to 10^4 ohm m to allow for sufficient diffusion of the IMF through the Moon and prevent unphysical pile-up at unmagnetized surfaces. *Sonnet* [1975] placed the resistivity of the lunar rock between 10^3 ohm m and 10^5 ohm m. The associated Reynolds number inside the Moon is then approximately 0.10, indicating that diffusion dominates that region. Numerical uncertainty can lead to numerical diffusion even in the region where η is set to zero. The Reynolds number associated with numerical diffusion is on the order of 10^4, and the region is thus dominated by convection.

[11] The dipole fields were created with two opposing current elements. The separation and depth of the current elements could be varied to change the characteristics of the surface field. The anomalous fields were assumed to be in the Southern Hemisphere at a latitude around 25°S. In the initial 2-D simulations, each of the dipoles that comprised the anomalous magnetic field were created with two opposing current elements placed at 26.1 and 78.3 km below the surface, respectively. This produced a magnetic field for a single dipole equal to 290 nT at the surface and 30 nT at 100 km. Additional dipoles can be added to increase the rate of fall-off of the magnetic field at high altitudes. The remainder of the MHD model is presented by *Harnett and Winglee* [2000], with the discussion of the expansion to nonideal MHD (MPD) discussed by *Harnett and Winglee* [2002].

[12] The simulations were run with either two or four dipoles present and with varying orientations for the dipole moments and field strengths. The dipole configurations are summarized in Table 1 for the cases with two dipoles and in Table 2 for the cases with four dipoles. The combination of multiple dipoles generates higher order magnetic moments. In the figures and tables the horizontal, or $\vec{x}$, axis is parallel to the ecliptic plane pointing away from the Sun. The vertical, or $\vec{z}$, axis is perpendicular to the ecliptic plane, with $+\vec{z}$ pointing in the direction of north. Radial vectors

Table 1. Dipole Parameters for the Results in Figure 1[a]

Figure	Depth, km	Dipole Moment	Surface Field, nT	Field at 100 km, nT
1a	60.9	+z	231	35.7
	52.2	+z	313	33.3
1b	60.9	−z	231	35.7
	52.2	−z	313	33.3
1c	26.1	−z	216	8.58
	17.4	+z	575	14.6
1d	26.1	+z	216	8.58
	17.4	−z	575	14.6

[a]The depth of the dipole is the depth of the midpoint between the two current elements that create the dipole field. The directions of the dipole moments ($\pm\vec{z}$) are all parallel to the vertical axis and the IMF ($-\vec{z}$). The dipoles are listed in decreasing z position and increasing x, thus the first dipole listed in each case is the dipole closest to the top of the simulation box, and conversely, the last dipole listed is closest to the bottom of the box. The magnetic field strengths are taken at points on a horizontal line through the dipole location.

originate from the center of the Moon. The resolution of the simulations in the regions shown is 8.7 km.

3. Two Dipoles

[13] When two dipoles, with dipole moments in the $+\vec{z}$ direction, are placed 150 km apart, the distance of the shock from the surface is nearly double the distance when only one of those dipoles is present (Figure 1a), while the general shape of the mini-magnetosphere remains the same. Directly opposite the lower dipole the shock surface forms 270 km above the surface, 42% higher than when the upper dipole was not present. In the downstream region the shock surface forms 225 km above the surface, an increase of 138% from when only one dipole is present. The lower dipole is at the same position as those in the single dipole simulations [*Harnett and Winglee*, 2000, 2002].

[14] The field strength is 91 nT at the surface halfway between the two dipoles and 29.5 nT at 100 km above the midpoint. The magnitude of the magnetic field magnitude at 100 km above the lower dipole is 32 nT and 313 nT at the surface (Table 1), both only 10% larger than with the single dipole in the previous results. Therefore the fall-off of the magnetic field with altitude, relative to the surface field, is similar in both the single dipole and double dipole cases. The increased size of the mini-magnetosphere is not due to a substantial increase in the total field strength but rather the increased lateral extent of the anomalous region.

[15] The temperature of the plasma inside the mini-magnetosphere is comparable to the case with only one dipole. The presence of the second dipole inhibits fluid flow but does not increase the heating of the plasma. When the plasma is diverted around one of the dipoles, it can encounter another dipole which prevents the plasma from simply flowing around the surface of the Moon, causing the plasma to stagnate. Since the inhibited flow also inflates the mini-magnetosphere, the plasma is not compressed as much which results in less heating, as the pressure and density can not build up. The pressure and density in the region in between the two dipoles is comparable to the values in the region directly opposite a single dipole as the inflation of the mini-magnetosphere reduces the build up of pressure and density. The stagnation point forms further downstream in the simulation with two dipoles, but the pressure and density at the stagnation point are also comparable to the values when only one dipole is present.

[16] In Figure 1b the two dipoles have the same location as in Figure 1a; the only difference is both dipole moments have been flipped 180° so that they are both pointing southward ($-\vec{z}$, direction). The anomalous surface field is now antiparallel to the IMF. The magnitude of the total anomalous magnetic field remains the same as in Figure 1a. The overall shape of the shock is similar to when only one dipole of the same orientation is present. The shock forms 100 km above the upper dipole and 120 km above the lower dipole, comparable to the height the shock formed above a single dipole of the same orientation. Instead of inflating the mini-magnetosphere above the anomalous region the inhibited fluid flow causes the shock in the downstream region to flair out such that between 150 and 500 km downstream the shock surface is 40% higher than when only one dipole is present.

[17] The density and pressure enhancements just directly opposite the upper dipole are similar to the values when only one dipole of the same orientation is present, while the enhancements opposite the lower dipole are 50% larger than for a single dipole. The significant increase in the density and pressure opposite the lower dipole is due to the presence of stagnant plasma. The density and pressure opposite the lower dipole are almost identical to the values at the stagnation point for one dipole, with the maximum density and pressure at the stagnation point in Figure 1b only 10% and 20% larger, respectively, than at the center of the stagnation point with one dipole. The stagnation point in both cases is caused by kinks in the reconnected magnetic field. With an increased anomalous magnetic field region, erosion of the anomalous field by the IMF is reduced and the inhibition of fluid flow by the total magnetic field is enhanced.

[18] The tail flares out owing to the additional magnetic field in the flank region and the increased build-up of

Table 2. Dipole Parameters for the Results in Figure 2[a]

Figure	Dipole Moment	Surface Field, nT	Field at 100 km, nT
2a	−z	205	6.34
	+z	223	13.8
	+z	185	14.0
	−z	229	14.6
2b	−z	354	11.2
	+z	399	16.0
	−z	390	2.71
	+z	388	14.5
2c	−x	135	5.12
	+x	150	11.2
	+x	118	11.4
	−x	155	11.9
2d	+r	111	7.00
	−r	186	13.7
	−r	75	16.2
	+r	124	14.0

[a]All the dipoles in 2a−2c are buried 26.1 km below the surface. The radial dipoles in 2d are buried between 28 and 43 km below the surface. The directions of the dipole moments are parallel to the horizontal axis and entry velocity of the solar wind ($+\vec{x}$), parallel to the vertical axis ($+\vec{z}$) and the IMF ($-\vec{z}$) or a radial vector originating at the center of the Moon ($\vec{r}$). The dipoles are listed in decreasing z position and increasing x, thus the first dipole listed in each case is the dipole closest to the top of the simulation box, and conversely, the last dipole listed is closest to the bottom of the box.

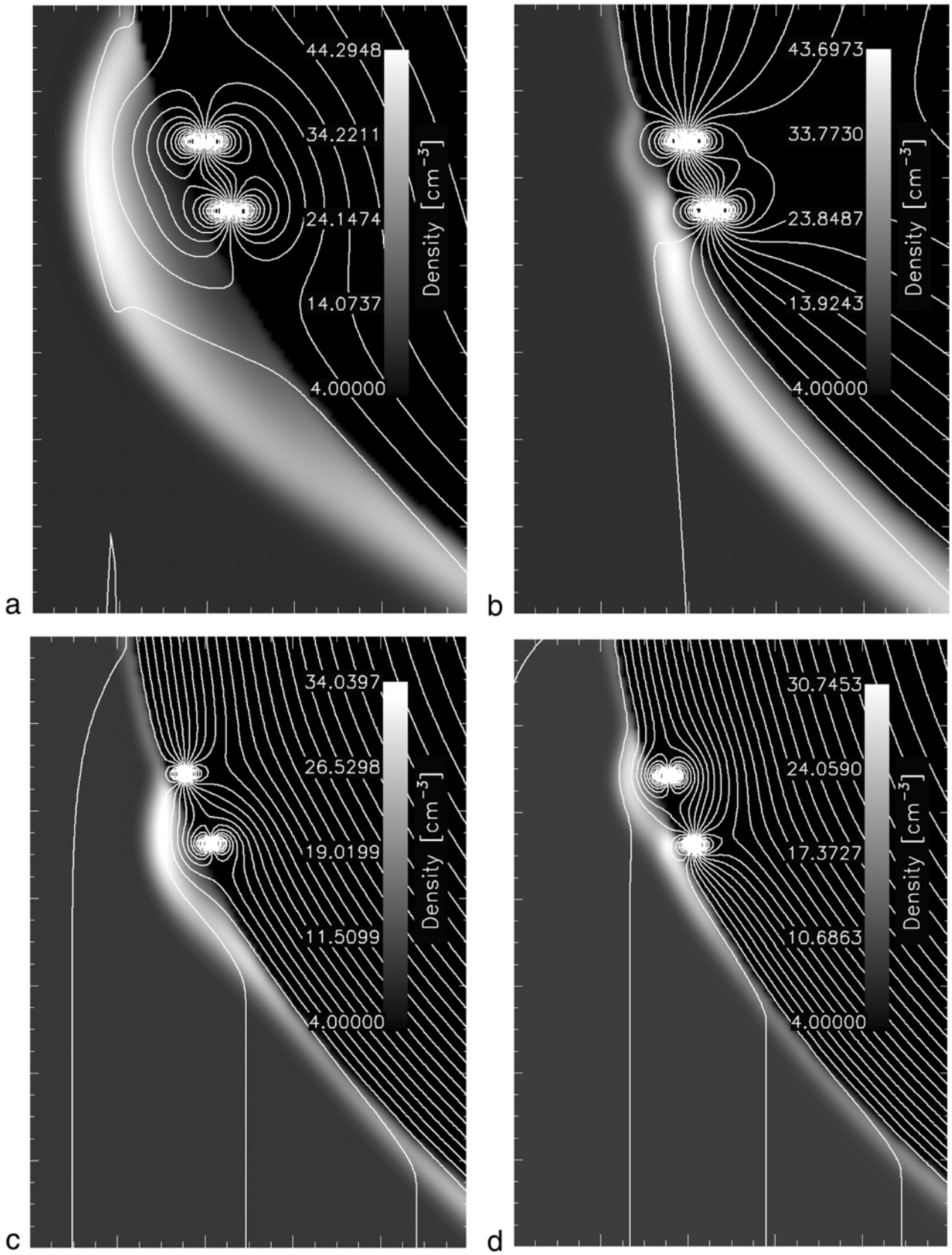
44.2948
34.2211
24.1474
14.0737
4.00000
Density [cm^{-3}]
a
43.6973
33.7730
23.8487
13.9243
4.00000
Density [cm^{-3}]
b
34.0397
26.5298
19.0199
11.5099
4.00000
Density [cm^{-3}]
c
30.7453
24.0590
17.3727
10.6863
4.00000
Density [cm^{-3}]
d

stagnant plasma. The enhanced stagnation point pushed the shock out directly below the anomalous region. That inflated shock surface is maintained further downstream by the enhanced anomalous field in the flank region. The polar magnetic field that drapes around the surface of the Moon is responsible for holding solar wind off the surface in the tail region and guiding it around the surface of the Moon. With the additional magnetic field in this region from the second dipole, there is a greater barrier between the solar wind and the lunar surface, causing the shock surface to form further from the surface.

[19] With two dipoles present, the anomalous magnetic field strength can be reduced while still causing a mini-magnetosphere to form at or above 100 km from the surface. In Figure 1c the two dipoles have opposing orientations. The upper dipole moment points in the southward (−z) direction while the lower dipole moment points in the northward (+z) direction. They are also now closer to the surface and the strength of the field, relative to the surface field, falls off faster. The magnetic field is 20 nT at the surface half way between the two dipoles and 8.26 nT at 100 km above the midpoint. The field strength at 120 km above the lower dipole is 7.5 nT. These values are much closer to measured values, particularly at 100 km above the surface, and less than the minimum magnetic field magnitude for which a shock would form with only one dipole present in the previous simulations [*Harnett and Winglee*, 2000].

[20] The outer shock surface in Figure 1c at its maximum height above the surface is 140 km when above the lower dipole. The upper dipole does little to hold plasma off the surface directly above its location, but it enhances the deflection of plasma by the lower dipole. The magnetic field from the upper dipole connects to the lower dipole field, expanding the lateral extent of field lines parallel to the IMF. Fluid below the upper dipole and above the lower dipole cannot impact the surface because of the magnetic field running tangential to the surface. This holds the plasma off the surface in the region between the two dipoles and inflates the size of the mini-magnetosphere.

[21] When only the direction of the dipole moments in Figure 1c are flipped by 180^o, the mini-magnetosphere changes shape and the height of the shock surface decreases (Figure 1d). The high point of the shock is 96 km above the surface. The dipole with a moment antiparallel to the IMF is primarily responsible for deflecting the solar wind since the surface field will be parallel to the IMF. Thus the decrease in shock height is primarily due to the smaller surface field strength at the dipole in the $+\vec{z}$ direction (i.e., top dipole). However, it is also due to how the two dipoles combine to deflect the plasma. The surface field at the lower dipole reconnects with the IMF, eroding the anomalous field and creating cusp-like structures that allow the plasma access to the surface. Most of the plasma that is deflected by the top dipole travels downward where it can either interact with the plasma held of the surface by the lower dipole, creating the stagnation point, or impact the surface.

[22] If the relative dipole field strengths in Figure 1d are reversed such that the surface field at the upper dipole is 400 nT and 100 nT at the lower dipole, but the dipole orientation remains the same, a shock forms 156 km above the upper dipole. The dipole with the moment in the $+\vec{z}$ direction remains the strongest dipole. The shock is round like the shock in Figure 1c, and no stagnation point forms above the lower dipole. The larger field strength at the upper dipole, relative to the lower dipole, means that the upper dipole deflects most of the plasma before it interacts with the lower dipole. Even with the smaller surface field, when compared with the cases in Figures 1c and 1d, this case forms the highest shock height owing to a slower fall-off of the field. The field strength at 100 km is approximately 18 nT, as opposed to 12 nT in the cases in Figures 1c and 1d.

[23] The slower fall-off in field strength leads to an increase in the lateral extent of the parallel surface field. In Figure 1c, the anomalous magnetic field is roughly parallel to the IMF for 222 km around the lower dipole. In Figure 1d, the lateral extent of parallel anomalous field around the upper dipole is only 187 km. The lateral extent is 226 km when the surface field in Figure 1d is 400 nT at the upper dipole and 100 nT at the lower dipole. It is this increase in lateral extent that causes inflation.

4. Four Dipoles

[24] When four dipoles are present on the surface, alternating dipoles are needed to create an anomalous magnetic field that is on the order of 300 nT at the surface and less than 10 nT at 100 km. This indicates that higher order moments are necessary to accurately model the magnetic field in region of plasma interaction. The largest surface fields with the fastest fall-off are for dipoles with moments aligned mostly parallel to the surface.

[25] In all of the four dipole simulations, the top dipole and the one second from the bottom are at the same location as the dipole pairs in the Figures 1c and 1d. The dipole field strengths and orientations are listed in Table 2.

[26] The maximum shock height in Figure 2a is 144 km. The field configuration creates a mini-magnetosphere similar in size and shape to both the case with two alternating dipoles in Figure 1c and a single dipole with the moment antiparallel to the direction of the IMF. However, in the case of the single dipole, the field strength at 100 km was 3 times larger, while the maximum shock height was only 40 km higher. The dipole moments of the two inner dipoles are aligned, creating a cumulative field that is dipole in nature. The two dipoles on the outer edges reconnect in such a way as to enhance the lateral extent of the field from the two inner dipoles. The cusp-like structure that forms around the

Figure 1. (opposite) Density plots and magnetic field lines for four different cases with two dipoles. The orientation and strength of the dipole fields are defines in Table 1. The moon has a constant density of 4.0 cm^{-3} and the solar wind a density of 10.0 cm^{-3}. The boxes contain an area 870 km by 1218 km, with each tick mark equal to 5 grid points or 43.5 km. The density contours were smoothed slight to reduce minor pixilation. The maximum value in the density corresponds to white on the color bar. (a) Slow fall-off of surface field, dipole moments: +z. (b) Slow fall-off of surface field, dipole moments: −z. (c) Opposing dipole moments. (d) Opposing dipole moments, 180° flip. See color version of this figure at back of this issue.

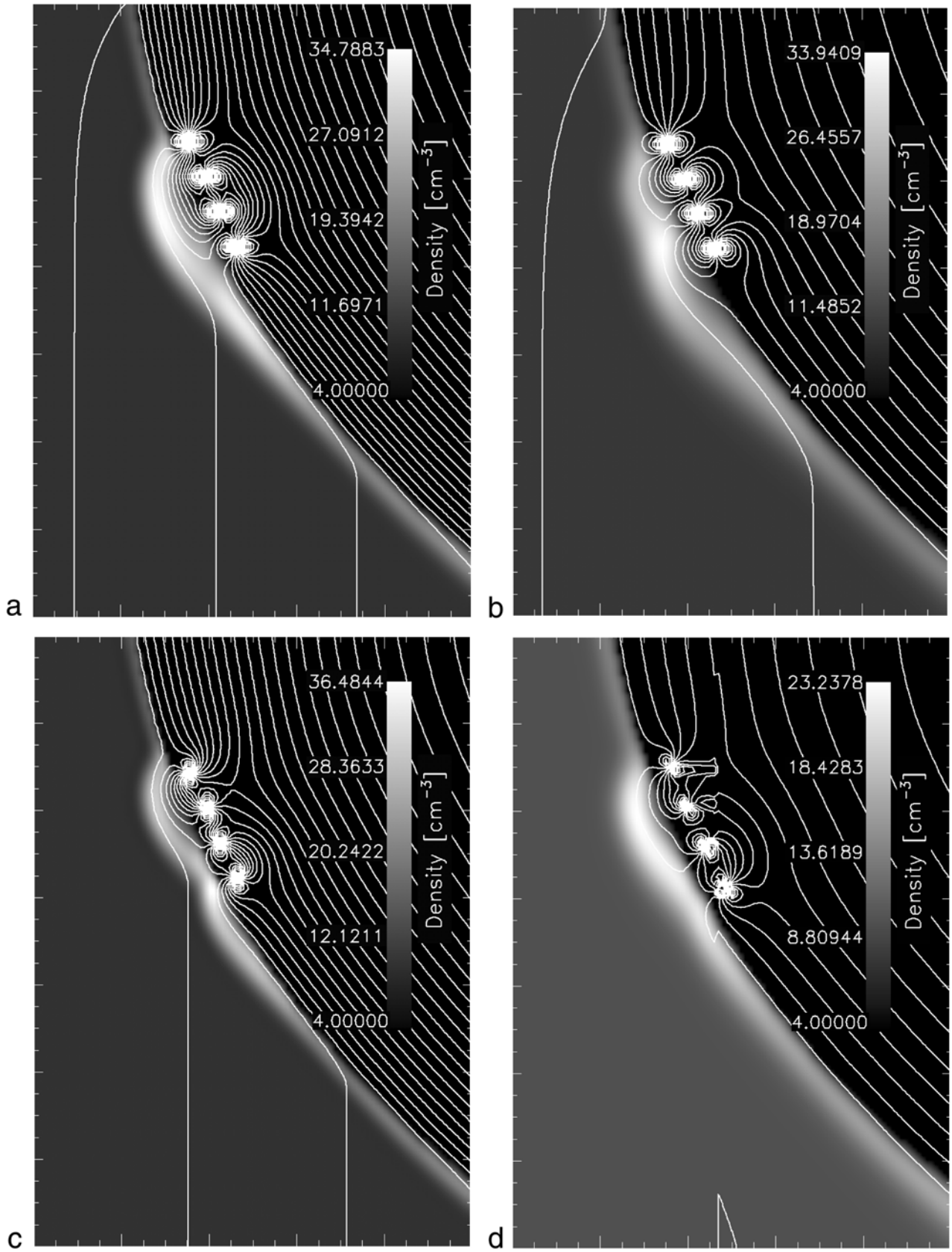

Figure 2. The figures are all of the same form as in Figure 1. The dipole configurations are defined in Table 2. The sharp kinks in the magnetic field lines in Figure 1d are due to numerical uncertainties in calculating the magnetic field lines for dipoles not aligned with one of the axes. (a) Inner dipole moments: +z, outer dipole moments: −z. (b) Alternating dipole moments. (c) Middle dipole moments: +x, outer dipole moments: −x. (d) Alternating radial dipole moments. See color version of this figure at back of this issue.

bottom dipole allows plasma access to the surface. Thus the pressure and density do not build up as much as in the surrounding areas.

[27] When no dipole moments are in the same direction as the neighboring dipoles (Figure 2b), the resulting shock is similar to the case with dipole moments parallel to the IMF (Figure 1b). However, unlike the case with the parallel dipoles, the tail in Figure 2b does not flair out. The maximum shock height is 157 km in a region downstream of all the dipoles.

[28] The stagnation point in Figure 2b comes about from the interaction of the two dipoles oriented in the +z direction. The top dipole reconnects with the dipole just below to increase the lateral scale, while dipole second from the top deflects the solar wind down towards the other dipoles. The bottom dipole deflects not only the solar wind but also the plasma directed downward by the upper dipoles, with some of the deflected plasma being directed upwards where it stagnates and inflates the shock surface.

[29] The stagnation point is not directly between the two dipoles in the +z direction due to the orientation of the dipole between them. The orientation of the middle dipole is in the −z direction leading to reconnection of the surface field to the IMF and allowing ambient plasma access to the surface, thereby reducing the build-up of pressure and density in that region.

[30] When the alternating dipoles are perpendicular to the IMF, the shape and size of the shock surface (Figure 2c) is very similar to the shock in Figure 1d. The reason for this is the alignment of the anomalous field with respect to the IMF. The anomalous field between the top two dipoles is parallel to the IMF, just like the surface field for a dipole moment antiparallel to the IMF (see the upper dipole in Figure 1d). The anomalous field between the two lower dipoles is antiparallel to the IMF, as it would be opposite a dipole moment parallel to the IMF. Thus the direction of the surface fields are similar in both Figure 1d and Figure 2c.

[31] The maximum shock height (opposite the upper two dipoles) in Figure 2c is 96 km above the surface with a stagnation point forming downstream, just as in the case with two dipoles. However, in the case with four dipoles, the stagnation point forms further down stream (192 km instead of 140 km) and causes the formation of a second bump in the shock surface due to larger density and pressure in the stagnation point.

[32] Another difference is that the magnitude of the magnetic field in the case with four dipoles is significantly smaller than in Figure 1d, 2–4 times smaller at the surface and 20%–40% smaller at 100 km above the surface. With two extra dipoles, the shock surface remains approximately the same size even though the magnitude of the magnetic field has been reduced. The field strength is smaller but the anomalous field is extended over a larger area leading to increased deflection of the solar wind, enhancing the shock region.

[33] The maximum pressure and density at the stagnation point in Figure 2c are 20% larger than the values at the stagnation point in Figure 1d owing to the magnetic field geometry above the lower dipoles. In Figure 1d, the magnetic field of the two dipoles, when combined, does elongate the magnetic field above the surface in the region between them. However, when the upper dipole deflects the solar wind down into the bottom dipole, the solar wind can still impact the surface above the lower dipole due to the cusp-like regions that form. Thus plasma will build up, but not to the extent it would if the reconnected magnetic field completely blocked access to the surface. With a denser concentration of dipoles in Figure 2c, the solar wind that is deflected around the upper three dipoles has decreased access to the surface in the region between the bottom dipole and the one above it.

[34] When the dipoles are in a radial direction (Figure 2d), similar to the horizontal orientation in Figure 2c, the maximum shock height is 135 km above the surface. The resulting magnetic field line geometry is similar to the horizontal orientation but the shock is 40 km higher for the radial dipoles. The shock around the radial dipoles is also 40 km higher than the shock in Figure 1d even though the magnitude of the magnetic field at the surface is considerably smaller in Figure 2d. The key difference is the slower fall-off of the total magnetic field with respect to the surface field for the radial dipoles (Table 2), leading to a total field strength at 100 km that is comparable to those in Figure 1d.

[35] The size and shape of the shock surface is heavily controlled by both the fall-off of the anomalous field and the size of the anomalous region. Since the magnetic field above the surface does not decrease with altitude as rapidly in Figure 2d as it does in Figure 2c, the plasma is deflected further above the surface, pushing the shock out. Also, the increase in size of the magnetized region from that in Figure 1d leads to a larger region over which the solar wind is deflected, also inflating the shock height.

5. Conclusion

[36] Mini-magnetospheres can be supported by magnetic anomalies near the lunar surface. Modeling the anomalous field with multiple dipoles leads to weaker fields above the surface but flow around the dipoles still leads to a bow shock forming well above the lunar surface. Inflation of the mini-magnetospheres is therefore not the result of an increase in the magnitude of the total field strength but rather an increase in the lateral extent over which the anomalous field occurs and the inhibited fluid flow that results. Plasma flowing around one dipole can encounter another dipole instead of freely flowing around the surface of the Moon or impacting the surface. As a result the plasma is slowed, causing stagnation and inflation. Thus mini-magnetospheres will form with smaller field strengths than previously estimated with only one dipole.

[37] Modeling the anomalous region with alternating multiple dipoles not only creates a total field that falls off faster with altitude due to the presence of higher order moments but also increases the lateral extent of the anomalous region. When the magnetic anomaly is modeled with four dipoles, the anomalous region is approximately 350–400 km in length. The large magnetic anomalies on the Moon are over 700 km in diameter [*Lin et al.*, 1998].

[38] These results indicate that the higher-order moments of the anomalous magnetic field not only contribute to deflecting the solar wind but also are largely responsible for determining the shape of the resulting mini-magnetosphere. Also, configurations with the similar magnetic field magnitude can produce mini-magnetospheres with vastly different sizes and shapes, since the direction of the resulting

magnetic field configuration relative to the IMF is as important as the interaction between individual dipole fields.

[39] While reduced from the single dipole approximation, the anomalous magnetic fields at 100 km above the surface in the multi-dipole simulations is still larger than the ~2 nT measured by Lunar Prospector (L. L. Hood, private communication, 2001). The next step in the investigation will be to extend the model to a full 3-D simulation. With all three spatial dimensions, a more realistic model of the extended anomalous regions can be incorporated into the simulations.

[40] **Acknowledgments.** This work was funded by a NASA Graduate Student Research Fellowship, NASA grants 61-9801 and 62-1693 and NSF grant ATM-9731951.

[41] Arthur Richmond thanks L. L. Hood and R. P. Lin for their assistance in evaluating this paper.

References

Freeman, J. W., Jr., Energetic ion bursts on the nightside of the Moon, *J. Geophys. Res.*, *77*, 239–243, 1972.

Harnett, E. M., and R. M. Winglee, Two-dimensional MHD simulations of the solar wind interaction with magnetic field anomalies on the surface of the Moon, *J. Geophys. Res.*, *105*, 24,997–25,007, 2000.

Harnett, E. M., and R. M. Winglee, 2.5-D particle and MHD simulations of mini-magnetospheres at the Moon, *J. Geophys. Res.*, *107*(A12), 1421, doi:10.1029/2002JA009241, 2002.

Hodges, R. R., The lunar atmosphere, *Icarus*, *21*, 415–426, 1974.

Hood, L. L., and C. R. Williams, The lunar swirls: Distribution and possible origins, *Proc. 19th Lunar and Planetary Science Conference*, 99–113, 1989.

Johnson, F. S., Lunar atmosphere, *Rev. Geophys.*, *9*, 813–823, 1971.

Lin, R. P., et al., Lunar surface magnetic fields and their interaction with the solar wind: Results from Lunar Prospector, *Science*, *281*, 1480–1484, 1998.

Neugebauer, M., et al., Solar wind observations of the Lunar surface with the Apollo-12 ALSEP, *Planet. Space Sci.*, *20*, 1577–1591, 1972.

Richtyer, R. D., and K. W. Morton, *Difference Methods for Initial Value Problems*, Wiley-Interscience, New York, 1967.

Sonnet, C. P., Solar wind induction and lunar conductivity, *Phys. Earth Planet. Inter.*, *10*, 313–322, 1975.

E. M. Harnett and R. M. Winglee, Department of Earth and Space Sciences, University of Washington, Box 351310, Seattle, WA 98195-1310, USA. (eharnett@ess.washington.edu; winglee@ess.washington.edu)

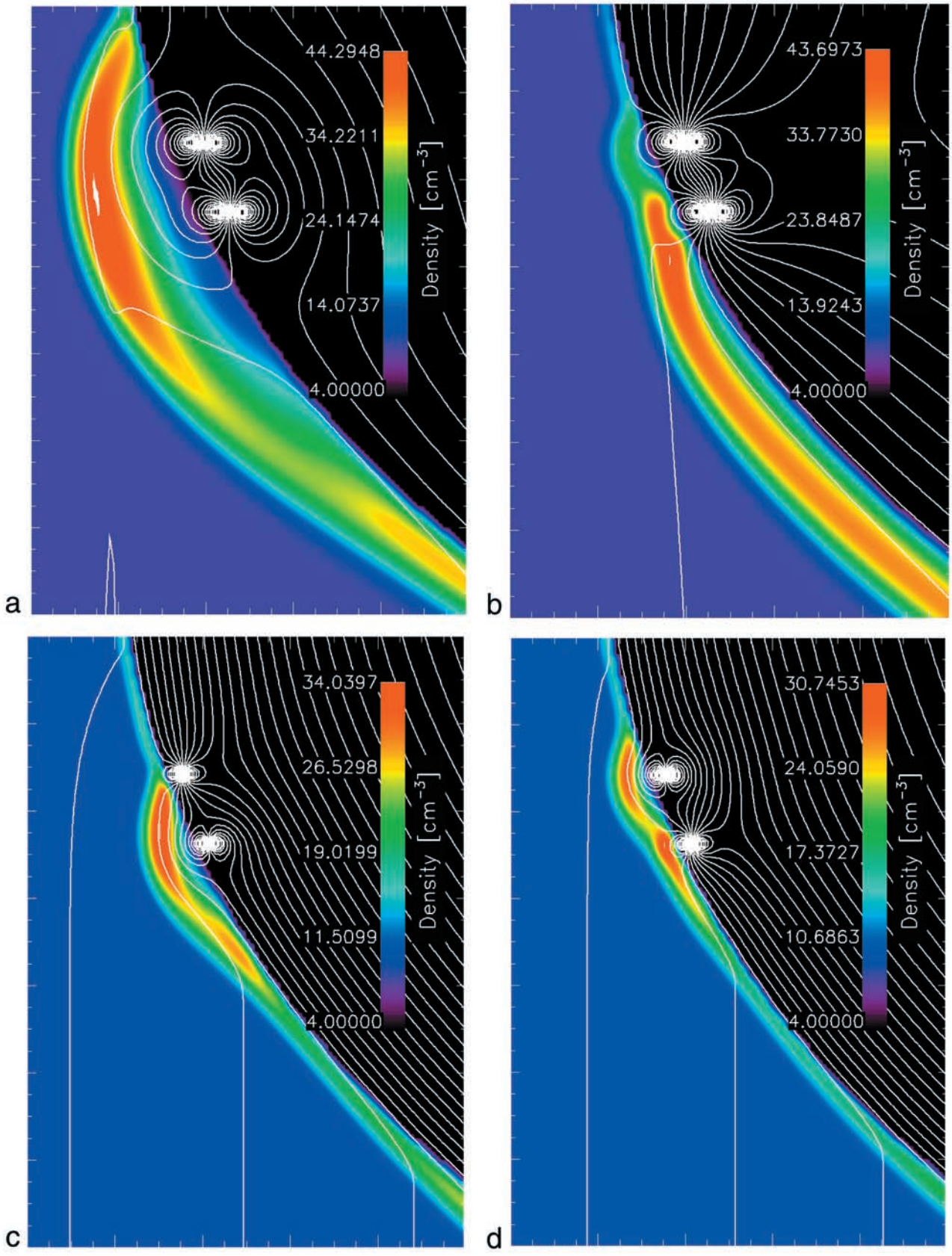
44.2948
34.2211
24.1474
14.0737
4.00000
Density [cm^{-3}]
a
43.6973
33.7730
23.8487
13.9243
4.00000
Density [cm^{-3}]
b
34.0397
26.5298
19.0199
11.5099
4.00000
Density [cm^{-3}]
c
30.7453
24.0590
17.3727
10.6863
4.00000
Density [cm^{-3}]
d

Figure 1. (opposite) Density plots and magnetic field lines for four different cases with two dipoles. The orientation and strength of the dipole fields are defines in Table 1. The moon has a constant density of 4.0 cm^{-3} and the solar wind a density of 10.0 cm^{-3}. The boxes contain an area 870 km by 1218 km, with each tick mark equal to 5 grid points or 43.5 km. The density contours were smoothed slight to reduce minor pixilation. The maximum value in the density corresponds to white on the color bar. (a) Slow fall-off of surface field, dipole moments: +z. (b) Slow fall-off of surface field, dipole moments: −z. (c) Opposing dipole moments. (d) Opposing dipole moments, 180° flip.

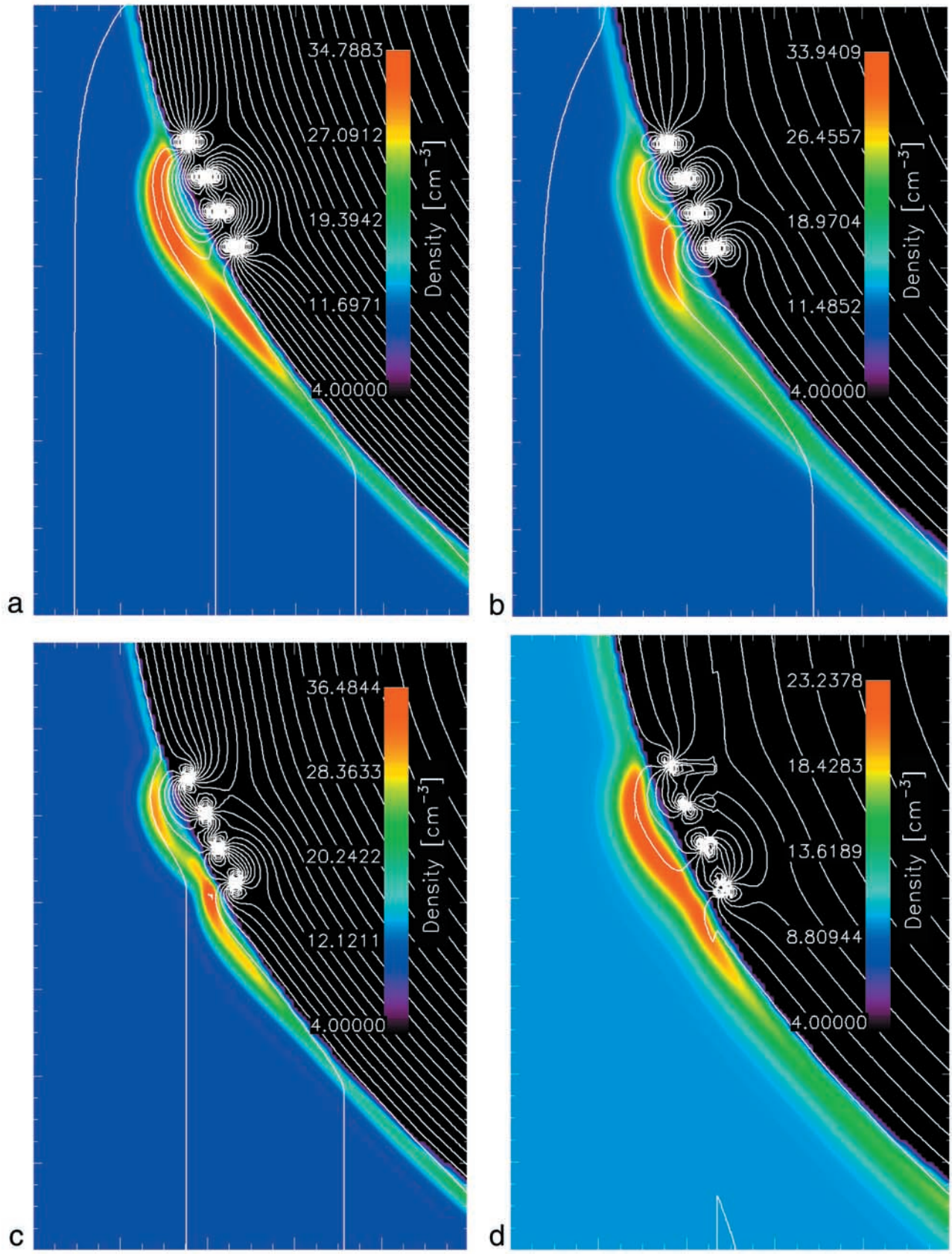

Figure 2. The figures are all of the same form as in Figure 1. The dipole configurations are defined in Table 2. The sharp kinks in the magnetic field lines in Figure 1d are due to numerical uncertainties in calculating the magnetic field lines for dipoles not aligned with one of the axes. (a) Inner dipole moments: +z, outer dipole moments: −z. (b) Alternating dipole moments. (c) Middle dipole moments: +x, outer dipole moments: −x. (d) Alternating radial dipole moments.